ORIGINAL PAPER

Parameterization of snow-free land surface albedo as a function of vegetation phenology based on MODIS data and applied in climate modelling

Diana Rechid · Thomas J. Raddatz · Daniela Jacob

Abstract The aim of this study was to develop an advanced parameterization of the snow-free land surface albedo for climate modelling describing the temporal variation of surface albedo as a function of vegetation phenology on a monthly time scale. To estimate the effect of vegetation phenology on snow-free land surface albedo, remotely sensed data products from the Moderate-Resolution Imaging Spectroradiometer (MODIS) on board the NASA Terra platform measured during 2001 to 2004 are used. The snow-free surface albedo variability is determined by the optical contrast between the vegetation canopy and the underlying soil surface. The MODIS products of the white-sky albedo for total shortwave broad bands and the fraction of absorbed photosynthetically active radiation (FPAR) are analysed to separate the vegetation canopy albedo from the underlying soil albedo. Global maps of pure soil albedo and pure vegetation albedo are derived on a 0.5° regular latitude/longitude grid, re-sampling the high-resolution information from remote sensing-measured pixel level to the model grid scale and filling up gaps from the satellite data. These global maps show that in the northern and mid-latitudes soils are mostly darker than vegetation, whereas in the lower latitudes, especially in semi-deserts, soil albedo is mostly higher than vegetation albedo. The separated soil and vegetation albedo can be applied to compute the annual surface albedo cycle from monthly varying leaf area index. This parameterization is especially designed for the land surface scheme of the regional climate model REMO and the global climate model ECHAM5, but can easily be integrated into the land surface schemes of other regional and global climate models.

1 Introduction

Land surface albedo is the ratio of solar radiation flux reflected at the surface to the total incoming solar radiation flux. It determines the energy budget of the earth's surface, which in turn modifies hydrological processes and regulates circulation patterns. Thus, it is an important parameter in modelling climate processes. Modelling studies have shown complex interactions between surface albedo, climate, and the biosphere (Dickinson and Hanson 1984; Rowntree and Sangster 1986; Lofgren 1995; Berbet and Costa 2003). Surface albedo is determined by the surface properties, depending on the angular and spectral distributions of the incident solar radiation. Bare soil albedo depends on the soil moisture content, surface roughness, and soil texture. The soil texture is determined by soil mineral composition and organic deposition. Vegetation canopy albedo depends on leaf area index (LAI), leaf angle distribution, leaf transmittance, and reflectance. The land surface albedo shows not only spatial variability but also temporal variations. This can be observed by field studies (Song 1999) and examined by remotely sensed data (Zhou et al. 2003). The largest temporal and spatial variations of surface albedo are caused by snow cover. In this study we solely refer to the albedo over snow-free land surfaces called "background albedo".

This study focuses on the monthly time scale. Over vegetated surfaces, the monthly variability of albedo is mainly caused by seasonally varying vegetation characteristics. In the study of Song (1999), the relationship between

D. Rechid (✉) · T. J. Raddatz · D. Jacob
Max-Planck-Institute for Meteorology,
Bundesstraße 53,
20146 Hamburg, Germany
e-mail: diana.rechid@zmaw.de

albedo and plant phenology was examined by field observations in prairie grassland and agricultural crops. The observed albedo showed clear changes during the phenology phases from green-up to peak greenness, dry down and senescence or harvesting stage. The study of Song (1999) also showed the difficulty to distinguish the seasonal variations in albedo caused by phenological changes from those caused by solar zenith angle depending on land cover type. To reduce the confounding effects of the seasonal varying solar zenith angle on surface albedo one should compare albedo values at the same solar zenith angle. In this study, these overlying effects on seasonal albedo changes are not distinguished. Only the white-sky albedo is analysed to yield surface albedo as a function of vegetation phenology. The variability due to plant phenology is determined by the optical contrast between the vegetation canopy and the underlying soil surface. Over bright-coloured soils vegetation cover reduces surface albedo whereas plants on dark soils increase surface albedo. During the annual cycle of vegetation development the vegetation density is changing. This can be expressed by the leaf area index (LAI), which is the projection of the one-sided leaf area to the ground area. Our motivation is to describe land surface background albedo as a dynamic function of the LAI, which is applied in most climate models to describe spatial and temporal variability of vegetation properties.

The land surface schemes of climate models often use background albedos without temporal variations. Thus, in the general circulation model (GCM) ECHAM5 (Roeckner et al. 2003) and the regional climate model (RCM) REMO (REgional MOdel, Jacob et al. 2001) the albedo over snow-free land surfaces was prescribed by tabular values only depending on land cover type (Hagemann et al. 1999). During the last years, the availability of high-quality satellite data with high spatial and temporal resolution increased which provides the opportunity to develop advanced land surface parameterizations. For example, the Moderate Resolution Imaging Spectroradiometer (MODIS) measurements facilitate the retrieval of surface albedo products and consistent products of vegetation characteristics (Lucht et al. 2000; Schaaf et al. 2002). The aim of this study was to develop a more realistic parameterization of the snow-free land surface albedo for the REMO RCM describing the monthly varying surface albedo as a function of vegetation phenology using MODIS data. At the same time a study of Liang et al. (2005) also used MODIS data to develop an improved dynamic-statistical parameterization for snow-free land surface albedo. This parameterization was designed for the Common Land Model (CLM, Dai et al. 2003; Bonan et al. 2002; Zeng et al. 2002). The CLM albedo scheme is quite complex and considers for the direct beam and diffuse radiation the visible and near-infrared

spectral bands using several parameters depending on soil and land cover type. The surface albedo parameterization of this study was especially designed for the land surface scheme of the REMO RCM and the ECHAM5 GCM, but can also be applied to other climate models with similar albedo schemes.

To estimate the effect of vegetation phenology on snow-free land surface albedo, remotely sensed data from the Moderate-Resolution Imaging Spectroradiometer (MODIS) on board the NASA Terra platform measured during 2001 to 2004 are used. We analysed MODIS products of the white-sky albedo for total shortwave broad bands and the fraction of absorbed photosynthetically active radiation (FPAR) as a parameter describing the temporal variability of vegetation characteristics. A linear regression method enables us to separate the vegetation albedo from the underlying soil albedo. Global maps of pure soil albedo and pure vegetation albedo are derived on a 0.5° regular latitude/longitude grid, which can be applied to compute the annual surface albedo cycle from monthly varying leaf area index. To sum up, our intention is to apply MODIS data products to develop an advanced parameterization of the snow-free land surface albedo for climate modelling re-sampling the high-resolution information from remote sensing-measured pixel level to the model grid scale and filling up gaps from the satellite data. The temporal variation of snow-free surface albedo is described as a function of vegetation phenology on a monthly time scale.

This paper is organised as follows: In Sect. 2 the data products from MODIS used in this study are presented. The data are prepared and analysed in Sect. 3 and applied to estimate the annual albedo cycle for climate modelling in Sect. 4. In Sect. 5 we give conclusions and a short outlook.

2 Data

2.1 MODIS albedo

Remotely sensed global land surface albedos are routinely provided by the Moderate-Resolution Imaging Spectroradiometer (MODIS) aboard the NASA Terra platform. The MODIS albedo algorithm adopts the linear Bidirectional Reflectance Distribution Function (BRDF) model to characterize the anisotropy of the global surface. The standard 1-km resolution MODIS BRDF/albedo products (called MOD43B) are documented in Strahler et al. (1999), Lucht et al. (2000), Schaaf et al. (2002) and in the MOD43 User's Guide, available at http://geography.bu.edu/brdf/userguide/. These products are provided to the user community by the Earth Resources Observation System (EROS) Data Center in the equal Integerized Sinusoidal projection (ISIN) and

can be downloaded from http://edcdaac.usgs.gov/modis/dataproducts.asp. These 1-km standard products are reprojected and aggregated to a latitude/longitude projection at 0.05° resolution (called MOD43) and analysed by Gao et al. (2005). Validation results show good agreement with field measurements within 10% (Liang et al. 2002; Jin et al. 2003a, b; Wang et al. 2004). Here, we use the white-sky albedo for total shortwave broad bands (MOD43C1), which is provided globally for every 16-day period from March 2000 to present. MODIS albedo observations are cloud-cleared and atmospherically corrected accompanied by quality flags that include the percentage of snow cover.

2.2 MODIS FPAR

The seasonal variation of vegetation cover is detected by the fraction of absorbed photosynthetically active radiation (FPAR) data from the same instrument MODIS/Terra. The MODIS LAI/FPAR products are composited over an 8-day period at 1-km spatial resolution projected on a sinusoidal grid (MOD15A2). Validation results show reasonable performance of the MODIS LAI/FPAR algorithm (Tan et al. 2005; Privette et al. 2002). For the retrieval of LAI and FPAR from surface reflectance, an algorithm based on the physics of radiative transfer in vegetation canopies was developed and implemented for operational processing with MODIS aboard Terra (Myneni et al. 2002). The data are distributed by the EROS Data Center from February 2000 to the present time. For each 1-km pixel the product file provides LAI, FPAR and two quality control variables. LAI and FPAR values are related to the land fraction of each pixel. A detailed description is available at http://cybele.bu.edu/modismisr/products/modis/-userguide.pdf.

3 Method

3.1 Data preparation

The MODIS land surface albedo data includes snow and water albedo of surfaces covered with snow, inland water, or coastal water. But for our method we need the albedo only related to snow-free land surfaces. Thus, snow and water albedos need to be excluded. First, the MODIS albedo data is reprojected to a 0.5° regular grid. The accompanying quality flag containing information about snow cover is used to mask out snow pixels. The information of land-sea distribution is taken from the GLCCD (U.S. Geological Survey 1997, 2002). If the land fraction of a grid point is below 0.2, the grid point is excluded from the analysis. For grid cells ranging between 0.2 and 0.8 land fraction, albedo values of the surrounding land grid points are interpolated with the inverse distance

weighting method. If land fraction exceeds 0.8, the albedo value is kept unchanged.

MODIS FPAR data is transferred from the 1-km ISIN to a regular latitude/longitude grid at 0.5° resolution. Myneni et al. (2002) advise users of the provisional nature of the products of year one of MODIS operation in view of changes to calibration, geolocation, cloud screening and atmospheric corrections. Therefore, we use the MODIS data from day 65 of the year 2001 to day 65 of the year 2004.

3.2 Data analysis

Up to 70 pairs of snow-free surface broadband albedo and FPAR values for every 16-day period are obtained for all global grid points, where data are available. The correlation between albedo and FPAR values is shown in Fig. 1. Positive correlations marked with red colours indicate regions where increasing vegetation cover raises surface albedo. Negative correlations marked with blue colours identify regions where increasing vegetation cover reduces surface albedo. Uncoloured grid points refer to non-vegetated regions or missing data.

In our method, the FPAR value is used as an indicator of the presence of vegetation. The total background surface albedo (a) results from the vegetation albedo (a_{canopy}), where vegetation is present, and the albedo of the soil (a_{soil}), where the underlying surface is visible:

$$a = a_{soil} \cdot (1 - fpar) + a_{canopy} \cdot fpar \qquad (1)$$

By linear regression of MODIS FPAR and total surface albedo data the vegetation albedo and soil albedo can be estimated. If there is no vegetation (FPAR=0), surface albedo is equal to soil albedo. If vegetation is present, the contrast between vegetation albedo and soil albedo defines the slope of albedo change.

The regression method delivers reasonable results under the following premises and predefined limits: The method is only applied at grid points, where at least three pairs of albedo and FPAR values are available and the absolute FPAR value changes at least by 0.1. Otherwise, the grid point is excluded from the method due to high uncertainty of the results. If no vegetation is present (FPAR always 0), soil albedo is set to the mean MODIS albedo. In the case of minor vegetation cover (FPAR always below 0.2), the linear regression method is used to estimate the soil albedo and vegetation albedo is set to missing value. In the case of major vegetation cover (FPAR always beyond 0.8), no information about the soil albedo can be observed from the satellite. Here, soil albedo is set to missing value and vegetation albedo is set to mean MODIS albedo. If the regression provides unrealistic results exceeding the lower limit 0.07 for water or the upper limit 0.7 for glacier ice, the respective grid points are also excluded from the method. The resulting global map of the soil albedo is presented in Fig. 2.

Fig. 1 Correlation between FPAR and albedo data from MODIS/Terra 2001–2004
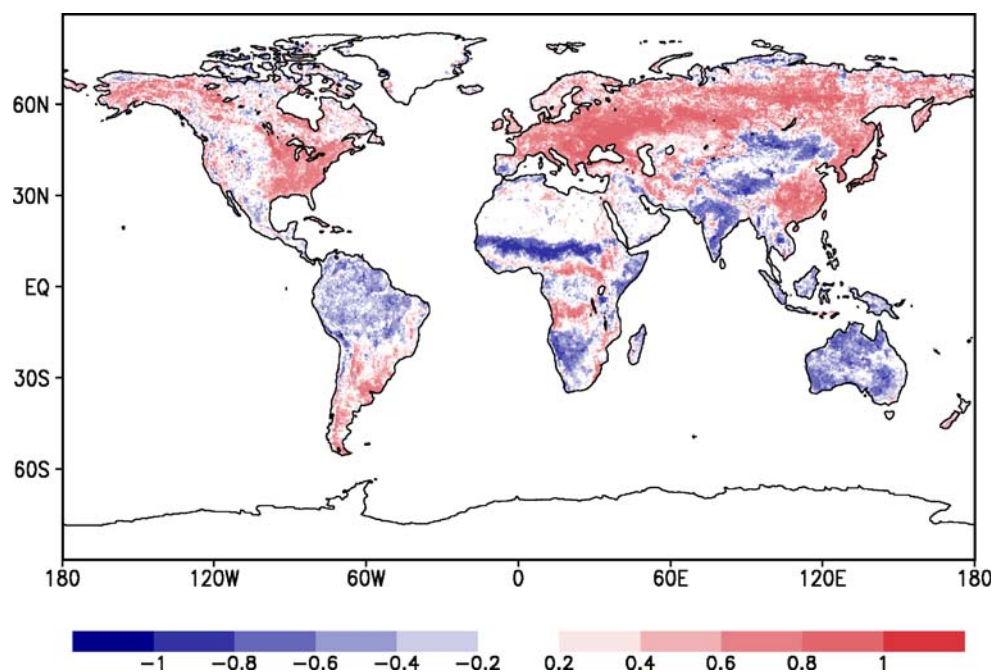
All missing grid points that are excluded from our method remain in white colour. Of a total of 60,606 ice-free vegetated land grid points, 7,869 grid points remain undefined, for 87% of the total grid points the method can be applied.

As climate models require surface information for each grid cell, soil albedo needs to be defined for all grid points. To complete our global map, grid points covered with glacier ice are identified by the Olson land cover types (Olson 1994a, b) and set to 0.7. Missing soil albedo values for grid points without glacier ice are spatially interpolated from the surrounding grid cells by inverse distance weighting

method. The same method is applied for missing vegetation albedo at vegetated grid points (FPAR beyond 0.2).

The soil albedo map shows that soils in the northern and mid-latitudes are predominantly dark with low albedo values. This can be understood by noting that low solar energy input and low surface temperatures in these regions slow down the decomposition of plant material and much organic material is stored in the soils. In contrast, surfaces in the lower latitudes often feature higher albedo values. In these regions, high input of solar radiation and high surface temperatures accelerate the mineralization of dead plant

Fig. 2 Global distribution of soil albedo at 0.5° resolution
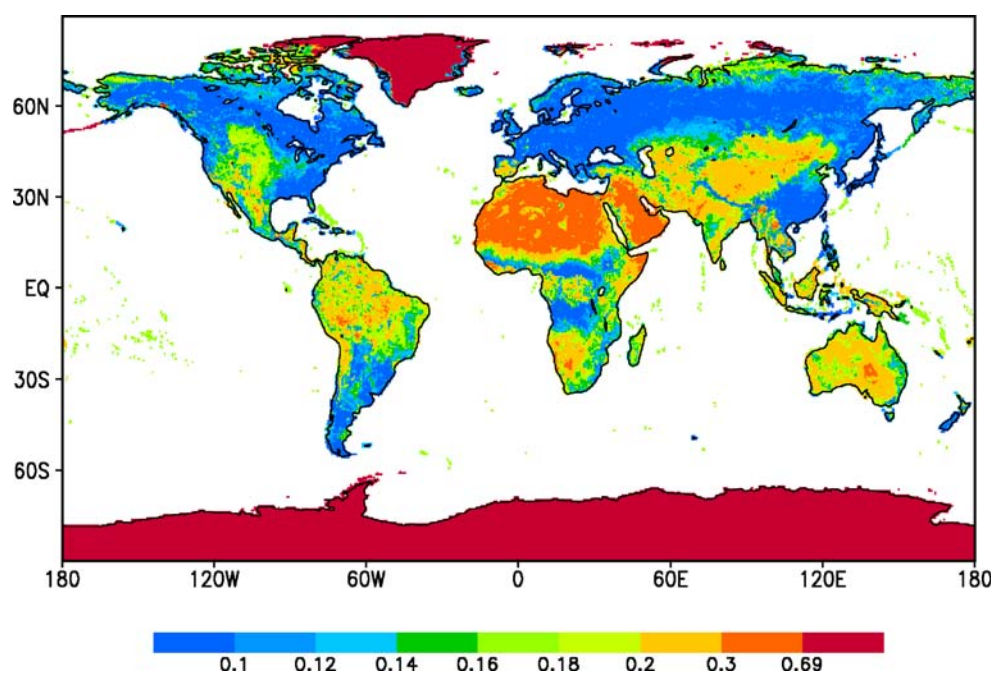
material and the content of organic material in the soils is quite low. Altogether, the soil albedo map shows realistic results, except for the northern part of South America. Here, in some places, soils show unrealistically high albedo values. This is possibly caused by undetected cloud and haze contaminations in the satellite data, but vegetation density is typically high in this region, so that nonetheless the total albedo is realistic. Figure 3 presents the result for the vegetation albedo. Most vegetation canopies feature albedo values between 0.1 and 0.15, but where grasses and crops are predominant (as in the mid-latitudes), vegetation canopies show higher albedo values. The boreal forests and the rain forests, in contrast, show quite low albedo values.

4 Annual background albedo cycle for climate modelling

The global distributions of soil and vegetation canopy albedo can be applied in climate modelling to describe the annual background albedo cycle as a function of vegetation phenology. In this study this method is adapted to the REMO RCM and the ECHAM5 GCM to prepare both models for testing the new albedo parameterization scheme both on the regional and the global scale.

4.1 Land surface representation and background albedo in REMO and ECHAM5

The general circulation model ECHAM5 and the regional climate model REMO use similar land surface schemes. The REMO RCM is based on the physical parameter-

izations of the ECHAM4 GCM. The land surface properties are represented by the same global dataset of land surface parameters LSP2 (Hagemann et al. 1999; Hagemann 2002). The LSP2 dataset is based on a global distribution of major ecosystem types (Global Land Cover Characteristics Database; GLCCD) according to a classification list of Olson (1994a, b). In REMO and ECHAM5 74 land use classes of the total 96 Olson ecosystem types are used (Hagemann 2002). The Olson ecosystem types were derived from Advanced Very High Resolution Radiometer AVHRR data at 1-km resolution supplied by the International Geosphere-Biosphere Program (Eidenshink and Faundeen 1994) and constructed by the U.S. Geological Survey (1997, 2002). For each land cover type mean parameter values for background surface albedo, fractional vegetation cover, minimum and maximum leaf area index and other vegetation properties are allocated. This information is aggregated to the model grid scale averaging the vegetation parameters of all land cover types, which are located in one model grid cell.

Together, so far, in ECHAM5 and REMO the albedo over snow-free land surfaces is defined by mean tabular values only depending on land cover type without temporal variability caused by changing soil properties as moisture content or changing vegetation properties as LAI or leaf colours. They are prescribed to the climate models as a lower boundary condition and remain constant during the whole model simulation.

The total surface albedo of a model grid box is the area-weighted linear average of the background albedo over the fraction with snow-free land, the albedo over the water fraction and the albedo over snow-covered grid area. The

Fig. 3 Global distribution of vegetation albedo at 0.5° resolution
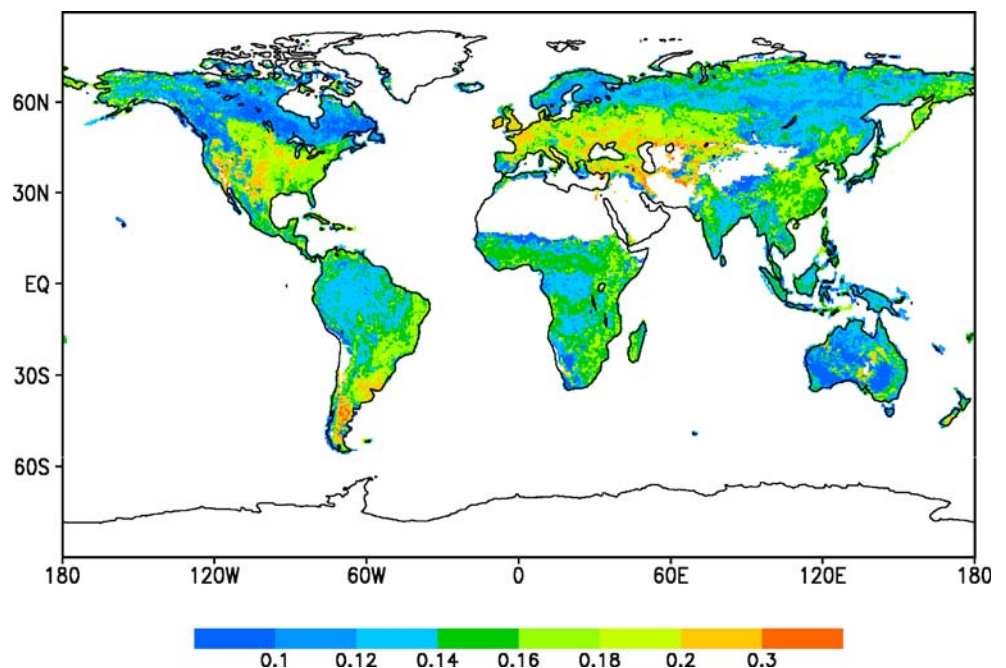
albedo over snow-covered land surfaces is a function of snow cover, temperature, forest fraction, subgrid-scale orography and in ECHAM5 also of the sky view factor depending on LAI.

In both the REMO RCM and the ECHAM5 GCM the total land surface albedo is the ratio of the solar radiation flux reflected at the surface to the total incoming solar radiation flux. So far, there is no spectral distinction for the reflection of the solar radiation at the surface, only the total shortwave broadband surface albedo is used. So, this spectral dependency is not considered in this study. Influencing the net radiation budget, the surface albedo has impact on the simulated vertical energy exchange at the earth's surface modifying surface heat fluxes and temperatures as well as hydrological processes. How the advanced albedo scheme will affect surface processes in the climate models is the topic of a further study (Rechid et al. 2008). There, the sensitivity of the simulated climate parameters in REMO and ECHAM5 to the new background albedo parameterization is evaluated in several global and regional climate simulations. The study investigates the individual performance of both models and how differently the new land surface background albedo scheme affects the simulations on the global and the regional scale.

The new background albedo parameterization describes the monthly varying background surface albedo as a function of vegetation phenology. In ECHAM5 and REMO, vegetation phenology is represented by the same monthly varying values of the leaf area index LAI (Roeckner et al. 2003; Rechid and Jacob 2006). These temporal varying vegetation fields are taken from the global dataset of land surface parameters LSP2 designed by Hagemann (2002). The seasonal variation of the LAI between minimum and maximum values is estimated by a global data field of the monthly growth factor, which is defined by climatologies of 2 m temperature and FPAR (Hagemann 2002). In regions with water availability being the limiting growing factor, the FPAR climatology is applied which considers indirectly the mean soil moisture conditions within the LAI variability. Together, this dataset provides a mean climatology of the annual LAI cycle without inter-annual variability.

So far, this mean seasonal LAI cycle was not related to temporal variability of snow-free land surface albedo. The LSP2 dataset also includes monthly fields of background albedo. This mean annual albedo cycle was derived by a method, which was designed for regions with bright soils where vegetation decreases the surface albedo, but this is not appropriate for the European region, the domain, where the REMO model is frequently applied. Here, dark soils are dominant, where vegetation increases the surface albedo (Bremicker 1998).

4.2 New background albedo scheme in REMO and ECHAM5

In ECHAM5 and REMO vegetation phenology is represented by a climatology of monthly varying values of the leaf area index LAI. Thus, we modify Eq. (1) converting the FPAR to LAI using a simple Beer's Law approach (Jarvis and Leverez 1983, cited in Turner et al. 2005):

$$fpar = 1 - e^{-K \cdot LAI} \qquad (2)$$

K is the canopy light extinction coefficient. As a simple approach K is assumed to be 0.5 for all vegetation types in this study. More sophisticated transformation algorithms are available (Chen et al. 1997; Gower et al. 1999), if they can be consistently parameterized within the land surface scheme of the climate model.

According to Eq. (1) we get the following function for the total land surface background albedo:

$$a = a_{soil} \cdot e^{-0.5 \cdot LAI} + a_{canopy} \cdot \left(1 - e^{-0.5 \cdot LAI}\right) \qquad (3)$$

In Fig. 4 the resulting annual mean of the climatological land surface background albedo for the climate models is presented. For comparison, the MODIS annual mean snow-free land albedo averaged over the whole period 2001–2004 is shown in Fig. 5. For the MODIS picture the annual means are displayed only for those grid points, where values are available for all months of the year. For the following comparisons between the annual background albedo cycles of the climate models and of MODIS only those defined MODIS grid points are comprised in the area-averages for the selected world regions, which are also presented in Figs. 4 and 5. For northern Asia, no albedo cycle is computed becasue for this region almost no MODIS data are available for the winter season. The annual mean background albedos of the models and MODIS show quite good agreement except for Australia and the northern part of southern America, where the values are underestimated at many grid points by our method. A more detailed analysis of these results will be done while evaluating the annual albedo cycles of the models and MODIS area-averaged over the selected regions.

As examples, the mean annual cycle of the leaf area index climatology and the resulting mean annual background albedo cycles of Europe and Australia, respectively, are shown in Fig. 6. The values of LAI and albedo are horizontal area-weighted averages for both regions. The pictures indicate that in Europe soils are mainly darker than vegetation; hence, albedo is increasing with increasing LAI. In Australia, in contrast, soils are brighter than vegetation and albedo is decreasing with increasing LAI.

The resulting mean annual background albedo cycles for the selected world regions are compared to the mean annual

Fig. 4 Resulting annual mean of global background surface albedo climatology at 0.5° horizontal resolution for the climate models. The selected world regions are numbered for: *1* northern America, *2* southern America, *3* Europe, *4* northern Africa, *5* central Africa, *6* southern Africa, *7* southern Asia, *8* Australia
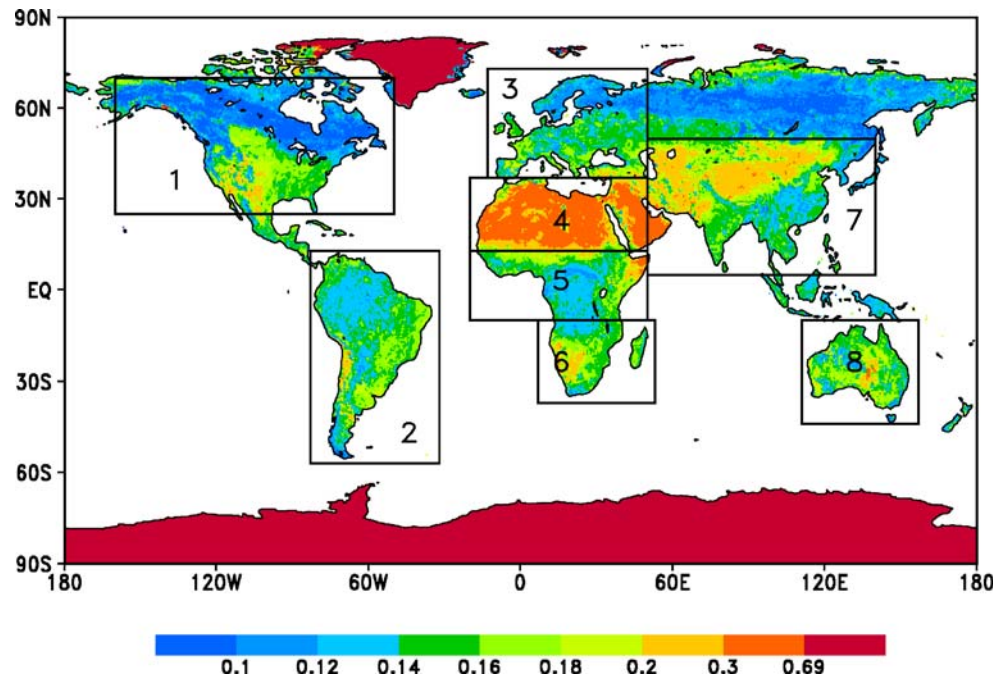
snow-free land albedo cycles of MODIS from 2001–2004 in Fig. 7. Additionally, the so far used annual mean background albedo of REMO and ECHAM5 from the LSP2 dataset is also displayed. In comparison to MODIS, the mean background albedo is overestimated by the LSP2 data. Hence, in almost all regions the new mean background albedo of the models is lower than the old LSP2 mean, which introduces partly a stronger change to the model albedo than the seasonal albedo variation.

Together, the observed MODIS albedo and the derived model albedo values show satisfying agreement. Especially,

in all African sub-regions and in southern America the background albedo values of the climate models fit very well to the MODIS albedo values. These are regions with only low temporal albedo variability. Moreover, these regions are dominated by natural land use types with low anthropogenic influence, which can be captured better by our method than regions with high anthropogenic influence. The other regions presented in Fig. 7 show some differences which shall be analysed and discussed in the following section.

Over Australia, the mean background albedo cycle is underestimated by our method for all months of the year.

Fig. 5 Annual mean of global snow-free land surface albedo at 0.5° horizontal resolution of MODIS averaged over the whole period 2001–2004. The selected world regions are numbered as in Fig. 4. Values are only plotted at grid points, where MODIS is available for all months of the year
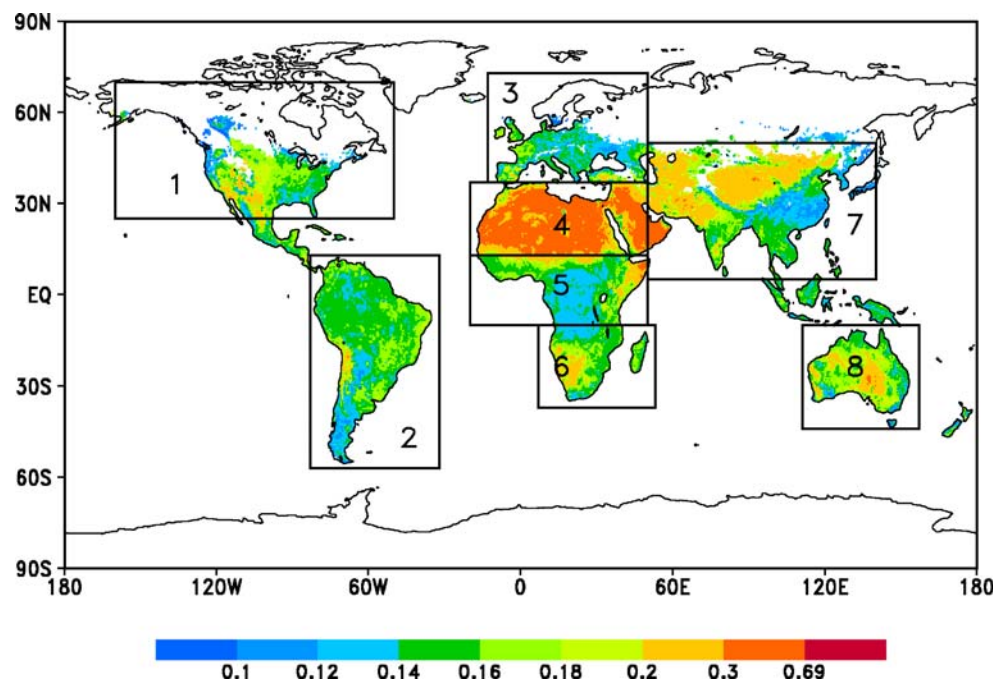
Fig. 6 Mean annual cycles of background albedo and LAI climatologies for Europe and Australia
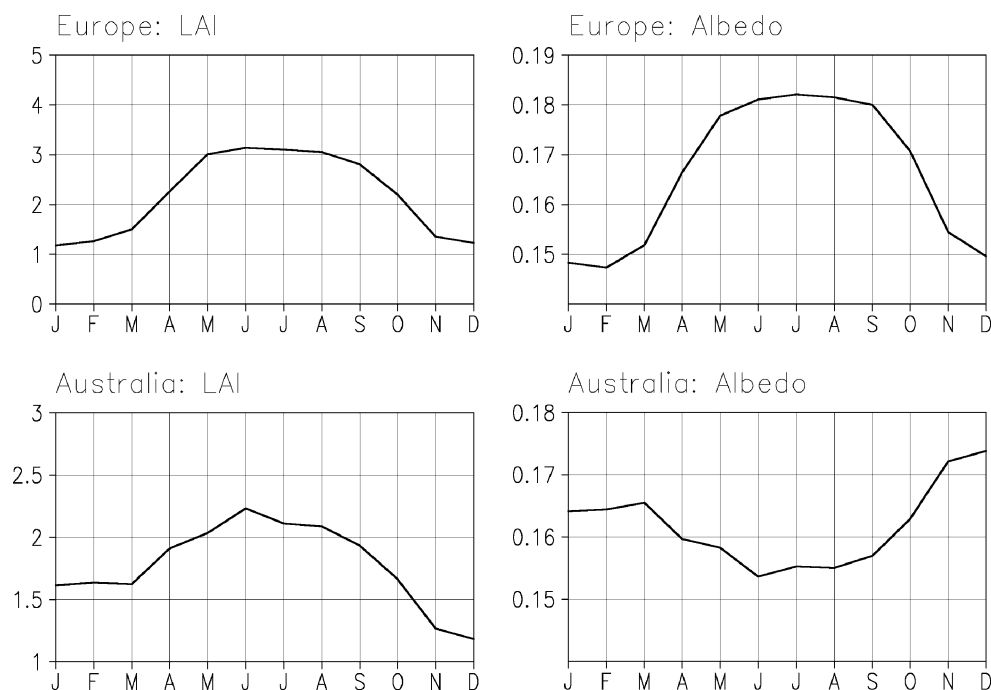
The temporal distribution is very similar, which means that the temporal variability of the LAI is correct, but there is an offset between the observed and the derived albedo cycle of about 0.02. This obviously results from an underestimation of the pure vegetation albedo in Australia by our method (compare Fig. 3.).

In northern America, Europe and northern Asia albedo increases during the summer months with increasing LAI. In southern Asia, the observed annual cycle of MODIS albedo is quite similar to that observed in northern America. The new albedo scheme correctly captures the annual mean albedo, but the annual cycle is not in agreement with the observed temporal variability. To analyse this we look at different parts of this region. In the northern parts with desert regions the background albedo is correct with constant values over the year. In South-east Asia, the albedo is increasing with higher LAI values during the summer months which is captured quite good by our method (not shown). The problem occurs over India. Here, the LAI is also increasing in summer with high precipitation during the Indian summer monsoon from June to September. As Fig. 2. and Fig. 3. show, in this region the pure vegetation albedo is lower than the underlying soil albedo. Additionally, the contrast is intensified due to the higher moisture content. This means that albedo would decrease with increasing vegetation density. However, neither the observed MODIS albedo nor the derived model albedo values decrease during summer. Here, possibly the MODIS data overestimates albedo due to undetected clouds with even increasing albedo values during the monsoon season. Thus, the derived albedo with constant values over the year is firstly satisfying.

The strongest seasonal albedo variations can be seen in Europe, where the optical contrast between the dark soils and the brighter vegetation canopy of grasses and crops is quite strong, but the new albedo keeps high during late summer, whereas MODIS albedo data decreases earlier. This is possibly due to variable vegetation albedo (changing colours of the leaves, for example), which cannot be considered by our method. Moreover, dominating agricultural land use types with high anthropogenic influence are difficult to capture within the albedo scheme as well as within the models' phenology scheme. This causes differences between the observed and the derived model albedo especially in Europe and also in Northern America.

5 Conclusions and outlook

Here, a method is developed to integrate high-resolution satellite information about the earth's surface consistently into the land surface schemes of the climate models REMO and ECHAM5. The annual albedo cycle of snow-free land surfaces is dynamically described as a function of the monthly varying LAI. This method can also be applied to vegetation models or to coupled climate-vegetation models within a fully dynamic phenology parameterisation.

We assumed that the monthly variation of land surface albedo is mainly caused by changes in vegetation cover. Another important factor causing seasonal variability of surface albedo is the soil moisture content. In our method, this is not explicitly considered, but in most cases, its effect is correlated with the vegetation cover. Thus, it is considered indirectly by the vegetation effect on surface

Fig. 7 New annual mean of the climatological background surface albedo cycle (*solid line*) in comparison to MODIS annual mean background surface albedo cycle averaged over the whole period 2001–2004 (*dotted line*) and LSP2 mean (*dashed line*) area-averaged over the land areas of the selected world regions
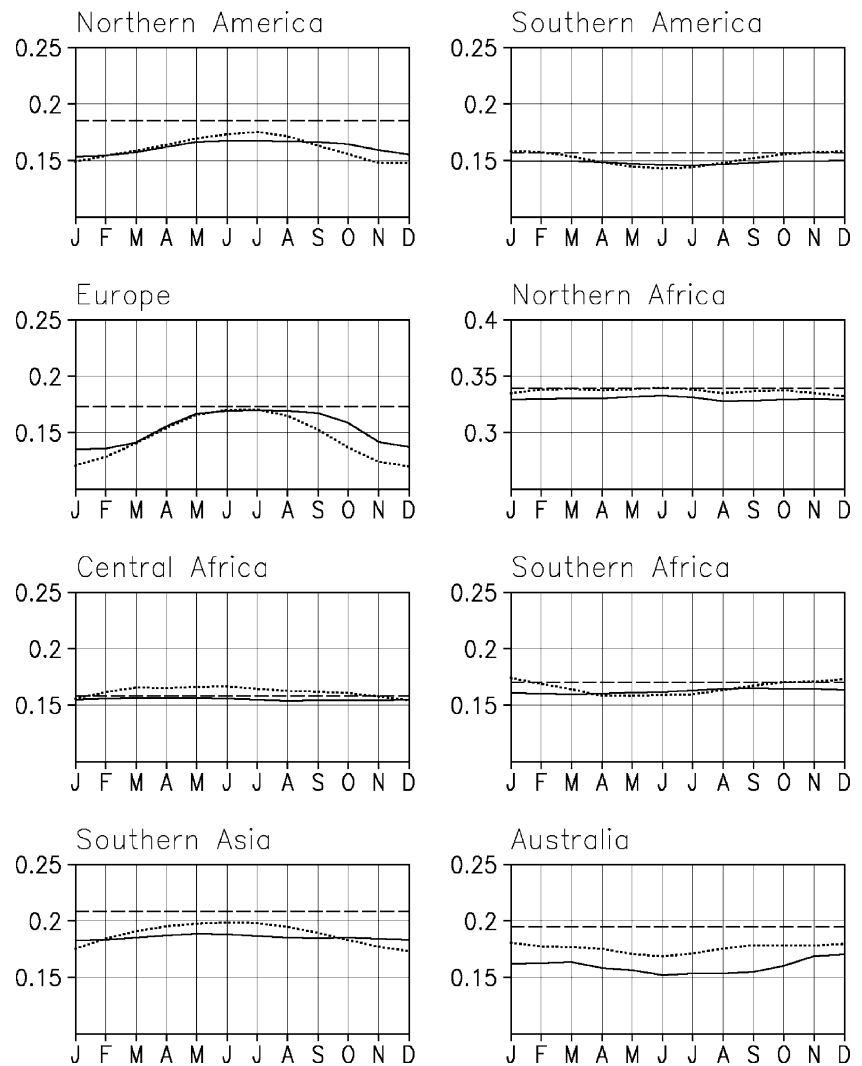
albedo. If the satellite products would also provide soil wetness data, this information could be included in our method to verify this assumption. A weak point of this study is, that only the "white-sky albedo" for the bi-hemispherical reflectance is taken into account while neglecting the "black-sky albedo" for the directional hemispherical reflectance, which strongly depends on the diurnal and seasonal variations of the solar zenith angle. Furthermore, albedos of different land cover types depend on the solar radiation spectrum. Whereas green canopies absorb much solar radiation in the visible interval (0.4–0.7 μm), they reflect and transmit most of the incident radiation in the near-infrared band (0.7–4.0 μm). So far, in the regional climate model REMO only the total shortwave broadband surface albedo is used. So, this spectral dependency is not considered in this study. However, for land surface schemes that distinguish visible and near-infrared surface albedos, the introduced method can be applied separately for the two spectral bands to advance the albedo parameterization.

In this study, the introduced method is adapted to the REMO RCM and the ECHAM5 GCM to prepare both models for testing the new albedo parameterization scheme both on the regional and the global scale. The resulting mean annual background albedo cycles of the climate models are compared to the snow-free land surface albedos of MODIS averaged over the whole time period from 2001–2004. Together, the comparison between MODIS and the new seasonal variations indicates realistic albedo cycles for the selected regions. The results show that the model's LAI is applicable in the introduced method. Applying the method to other models and LAI datasets, respectively, it is crucial to know that currently available LAI datasets differ strongly, which can lead to quite different results. How the advanced albedo scheme will affect surface processes in the climate models is the topic of a further study (Rechid et al. 2008). There, the sensitivity of the simulated climate parameters in REMO and ECHAM5 to the new background albedo parameterization is evaluated in several global and regional climate simulations.

Moreover, for the regional climate model REMO a dynamic vegetation phenology scheme for the LAI as a function of the model climate is currently developed. The so far used climatological mean annual LAI cycle does not account for inter-annual variability caused by changing thermal and moisture conditions from year to year. The new approach will no longer prescribe the monthly LAI values as a climatological boundary condition to the climate model but will compute daily LAI values prognostically during the model simulations as a function of the actual simulated temperatures and moisture parameters. As in our method, the background albedo is dynamically described as a function of the LAI, the advanced albedo scheme can be applied to this new phenology scheme and is expected to provide more realistic land surface albedo values on the daily time scale.

References

Berbet MLC, Costa MH (2003) Climate change after tropical deforestation: seasonal variability of surface albedo and its effects on precipitation change. J Clim 116:2099–2104

Bonan GB, Oleson KW, Vertenstein M, Levis S, Zeng X, Dai Y, Dickinson RE, Yang ZL (2002) The land surface climatology of the Community Land Model coupled to the NCAR Community Climate Model. J Clim 15:3123–3149

Bremicker M (1998) Aufbau eines Wasserhaushaltmodells für das Weser- und Ostsee-Einzugsgebiet als Baustein eines Atmosphären-Hydrologie-Modells. Dissertation an der Geowissenschaftlichen Fakultär der Albert-Ludwigs-Universität Freiburg, pp 36

Chen JM, Rich PM, Gower ST, Norman JM, Plummer S (1997) Leaf area index of boreal forests: theory, techniques, and measurements. J Geophys Res 102:29429–29444, DOI 10.1029/97JD01107

Dai Y, Zeng X, Dickinson RE, Baker I, Bonan GB, Bosilovich MG, Denning AS, Dirmeyer PA, Houser PR, Niu G, Oleson KW, Schlosser CA, Yang ZL (2003) The Common Land Model. Bull Am Meteorol Soc 84:1013–1023

Dickinson RE, Hanson B (1984) Vegetation-albedo feedbacks. In: Hanson JE, Takahashi T (eds) Climate processes and climate sensitivity. Geophys Monogr Ser, 29. AGU, Washington, DC, pp 180–186

Dickinson RE, Henderson-Sellers A, Kennedy PJ (1993) Biosphere-Atmosphere Transfer Scheme (BATS) version le as coupled to theNCAR Community Model. NCAR Tech. Note NCAR/TN-387+STR, 72pp., Natl. Cent. for Atmos. Res., Boulder, Colorado

Eidenshink JC, Faundeen JL (1994) The 1-km AVHRR global land dataset: first stages in implementation. Int J Remote Sens 15:3443–3462

Gao F, Schaaf CB, Strahler AH, Roesch A, Lucht W, Dickinson R (2005) MODIS bidirectional reflectance distribution function and albedo Climate Modeling Grid products and the variability of albedo for major global vegetation types. J Geophys Res 110: D01104, DOI 10.1029/2004JD005190

Gower ST, Kucharik CJ, Norman JM (1999) Direct and indirect estimation of leaf area index, fAPAR and net primary production of terrestrial ecosystems. Remote Sens Environ 70:29–51

Hagemann S, Botzet M, Dümenil L, Machenhauer M (1999) Derivation of global GCM boundary conditions from 1 km land use satellite data. Report 289, Max-Planck-Institute for Meteorology, Hamburg

Hagemann S (2002) An improved land surface parameter dataset for global and regional climate models. Report 336, Max-Planck-Institute for Meteorology, Hamburg

Jacob D, Podzun R (1997) Sensitivity studies with the regional climate model REMO. Meteorol Atmos Phys 63:119–129

Jacob D, Andrae U, Elgered G, Fortelius C, Graham PL, Jackson SD, Karstens U, Koepken C, Lindau R, Podzun R, Rockel B, Rubel F, Sass HB, Smith RND, Van den Hurk BJJM, Yang X (2001) A comprehensive model inter-comparison study investigating the water budget during the BALTEX-PIDCAP period. Meteorol Atmos Phys 77:19–43

Jarvis PG, Leverez JW (1983) Productivity of temperate deciduous and evergreen forests. In: Lange OL, Nobel PS, Osmond CB, Ziegler H (eds) Ecosystem process: mineral cycling, productivity and man's influence. Physiolog Plant Ecol, New series, Vol. 12D. Springer,Berlin Heidelberg New York, pp. 233–280

Jin Y, Schaaf CB, Gao F, Li X, Strahler AH, Lucht W, Liang S (2003a) Consistency of MODIS surface bidirectional reflectance distribution function and albedo retrievals: 1. Algorithm performance. J Geophys Res 108(D5):4158, DOI 10.1029/2002JD002803

Jin Y, Schaaf CB, Woodcock CE, Gao F, Li X, Strahler AH, Lucht W, Liang S (2003b) Consistency of MODIS surface bidirectional reflectance distribution function and albedo retrievals: 2. Validation. J Geophys Res 108(D5):4159, DOI 10.1029/2002JD002804.002804

Liang S, Fang H, Chen M, Shuey CJ, Walthall C, Daughtry C, Morisette J, Schaaf C, Strahler A (2002) Validating MODIS land surface reflectance and albedo products: methods and preliminary results. Remote Sens Environ 83:149–162

Liang X-Z, Xu M, Gao W, Kunkel K, Slusser J, Dai Y, Min Q, Houser PR, Rodell M, Schaaf CB, Gao F (2005) Development of land surface albedo parameterization based on Moderate Resolution Imaging Spectroradiometer (MODIS) data. J Geophys Res 110: D11107, DOI 10.1029/2004JD005579

Lofgren BM (1995) Surface albdo-climate feedback simulated using two-way coupling. J Clim 8:2543–2562

Lucht W, Schaaf CB, Strahler AH (2000) An algorithm for the retrieval of albedo from space using semiempircal BRDF models. IEEE Trans Geosci Remote Sens 38(2):977–998

Myneni RB, Hoffman S, Knyazikhin Y, Privette JL, Glassy J, Tian Y, Wang Y, Song X, Zhang Y, Smith GR, Lotsch A, Friedl M, Morisette JT, Votava P, Nemani RR, Running SW (2002) Global products of vegetation leaf area and fraction absorbed PAR from year one of MODIS data. Remote Sens Environ 83:214–231

Olson JS (1994a) Global ecosystem framework: definitions. USGS EROS Data Center Internal Report, Sioux Falls, SD, p 37

Olson JS (1994b) Global ecosystem framework: translation strategy. USGS EROS Data Center Internal Report, Sioux Falls, SD, p 39

Privette JL, Myneni RB, Knyazikhin Y, Mukelabai M, Roberts G, Tian Y, Wang Y, Leblanc SG (2002) Early spatial and temporal validation of MODIS LAI product in the Southern Africa Kalahari. Remote Sens Environ 83:232–243

Rechid D, Jacob D (2006) Influence of monthly varying vegetation on the simulated climate in Europe. Meteorol Z 15:99–116

Rechid D, Hagemann S, Jacob D (2008) Sensitivity of climate models to seasonal variability of snow-free land surface albedo. Submitted to Theor Appl Climatol (in press)

Roeckner E, Bäuml G, Bonaventura L, Brokopf R, Esch M, Giorgetta M, Hagemann S, Kirchner I, Kornblueh L, Manzini E, Rhodin A, Schlese U, Schulzweida U, Tompkins A (2003) The atmospheric general circulation model ECHAM-5: Part I. Model description. Report 349, Max-Planck-Institute for Meteorology, Hamburg

Roesch A, Wild M, Gilgen H, Ohmura A (2001) A new snow cover fraction parameterization for the ECHAM4 GCM. Clim Dyn 17:933S–946S

Rowntree PR, Sangster AB (1986) Modelling the impact of land surface changes on Sahel rainfall. Rep. 9, World Climate Research Programme, Geneva

Schaaf CB, Gao F, Strahler AH, Lucht W, Li X, Tsang T, Strugnee N, Zhang XY, Jin Y, Muller JP, Lewis P, Barnsley M, Hobson P, Disney M, Roberts G, Dunderdale M, Doll C, d'Entremont RP, Hu B, Liang S, Privette JL (2002) First operational BRDF, albedo and nadir reflectance products from MODIS. Remote Sens Environ 83:135–148

Song J (1999) Phenological influences on the albedo of prairie grassland and crop fields. Int J Biometeorol 42:153–157

Strahler AH, Lucht W, Schaaf CB, Tsang T, Gao F, Li X, Muller JP, Lewis P, Barnsley MJ (1999) MODIS BRDF/albedo product: algorithm theoretical basis document. NASA EOS-MODIS document, v5.0, NASA Goddard Space Flight Cent., Greenbelt, Md., p 53

Tan B, Hu J, Zhang P, Huang D, Shabanov N, Weiss M, Knyazikhin Y, and Myneni RB (2005) Validation of Moderate Resolution Imaging Spectroradiometer leaf area index product in croplands of Alpilles, France. J Geophys Res 110:D01107, DOI 10.1029/2004JD004860.0

Turner DP, Ritts WD, Cohen WB, Maeirsperger TK, Gower ST, Kirschbaum AA, Running SW, Zhao M, Wofsy SC, Dunn AL, Law BE, Campbell JL, Oechel WC, Kwon HJ, Meyers TP, Small EE, Kurc SA, Gamon JA (2005) Site-level evaluation of satellite-based global terrestrial gross primary production and net primary production monitoring. Glob Chang Biol 11:666–684

US Geological Survey (1997) Global land cover characteristics data base. http://edcwww.cr.usgs. gov/landdaac/glcc/globe_int.html

US Geological Survey (2002) Global land cover characteristics data base version 2.0. http://edcdaac.usgs.gov/glcc/globedoc2_0.html

Wang K, Liu J, Zhou X, Sparrow M, Ma M, Sun Z, Jiang W (2004) Validation of the MODIS global land surface albedo product using ground measurements in a semidesert region on the Tibetan Plateau. J Geophys Res 109:D05107, DOI 10.1029/2003JD004229229

Zeng X, Shaikh M, Dai Y, Dickinson RE, and Myneni R (2002) Coupling of the Common Land Model to the NCAR Community Climate Model. J Clim 15:1832–1854

Zhou L, Dickinson RE, Tian Y, Zeng X, Dai Y, Yang ZL, Schaaf CB, Gao F, Jin Y, Strahler A, Myneni RB, Yu H, Wu W, Shaikh M (2003) Comparison of seasonal and spatial variations of albedos from Moderate-Resolution Imaging Spectroradiometer (MODIS) and Common Land Model. J Geophys Res 108:D15, 4488, DOI 10.1029/2002JD003326